

Supplementary Information for

Surface Anchored Atomic Cobalt-Oxide Species Coupled with Oxygen Vacancies Boost the CO- Production Yield of Pd Nanoparticles

Dinesh Bhalothia,^a Shou-Shiun Yang,^a Che Yan,^a Amisha Beniwal,^a You-Xun Chang,^a Shun-Chi Wu,^a Po-
Chun Chen,^b Kuan-Wen Wang ^c,and Tsan-Yao Chen ^{a,d*}

Affiliations:

^a Department of Engineering and System Science, National Tsing Hua University, Hsinchu 30013, Taiwan

^b Institute of Materials Science and Engineering, National Taipei University of Technology, Taipei 10608, Taiwan.

^c Institute of Materials Science and Engineering, National Central University, Taoyuan 320, Taiwan

^d Hierarchical Green-Energy Materials (Hi-GEM) Research Centre, National Cheng Kung University, Tainan 70101, Taiwan

Corresponding Author:

Tsan-Yao Chen

Email: chencaeser@gmail.com

Tel: +886-3-5715131 # 34271

FAX: +885-3-5720724

1. Details for the synthesis of Pd-AC

The Pd-AC sample was prepared via wet chemical reduction method. Prior to synthesis, the catalyst carrier (i.e. carbon black; UR-XC72, UniRegion Bio-Tech) was surface functionalized for improving the metal-support interaction and uniform dispersion. Subsequently, in the 1st step, 6 g (1 wt.% solution in D.I. water and Polyvinylpyrrolidone (PVP); i.e. the actual amount of carbon black powder is 60 mg) of surface-functionalized carbon black (denoted as active carbon (AC)) was dispersed in 3.06 g of an aqueous solution containing 0.1 M palladium (II) chloride (99%, PdCl₂, Sigma-Aldrich Co.) and stirred at 600 rpm for 6 h at 25°C (solution A). The Pd precursor solution was prepared by dissolving palladium chloride (PdCl₂, 99%, Sigma-Aldrich Co.) in 1.0 M of HCl_(aq). The solution “A” (i.e. Pd²⁺ ions adsorbed on the surface of AC; Pd²⁺-^{ads}-AC) contains 18 mg of Pd²⁺ ions with a weight ratio of 30 wt.% to AC. In the 2nd step, a 10 ml of D.I. water solution consisting of 0.05 g of sodium borohydride (NaBH₄; 99%, Sigma-Aldrich Co.) was instantly dropped into the solution “A” and stirred at 600 rpm for 10 s to form the metastable Pd metal NPs on the AC surface (solution B). The final product (i.e. Pd-AC) was sequentially washed with acetone, ethanol and D.I. water, centrifuged, and dried at 120°C for 12 h.

2. Physical Characterizations of Experimental Nanocatalysts.

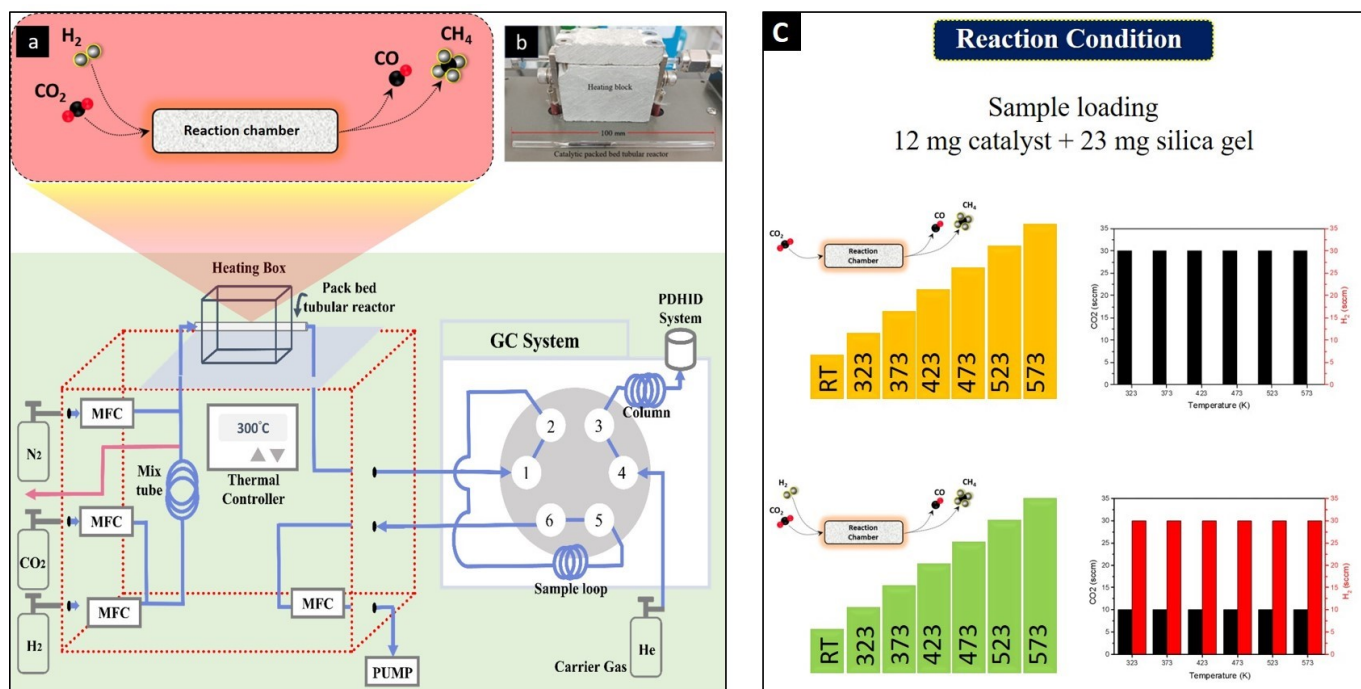
The physical properties of CoPd-CoO_{OV} as well as reference samples were investigated by the cross-referencing results of electron microscopy and X-ray spectroscopic techniques. The high-resolution transmission electron microscope (HRTEM) images were obtained at the National Tsing Hua University, Taiwan for revealing the crystal structure and surface morphology of as-prepared samples. The XRD spectra were measured at the beamline of BL-01C2 of the National Synchrotron Radiation Research Center (NSRRC), Taiwan with an incident X-ray of wavelength 0.6888 Å (18.0 KeV). The X-ray absorption spectroscopy (XAS) of experimental samples was executed at beamlines BL-17C and 01C1 of NSRRC, Taiwan and normalized by using ATHENA software. For the extended X-ray absorption fine structure (EXAFS) analysis, the backgrounds of the pre-edge and the post-edge were subtracted and normalized to the edge jump step from the XAS spectra. The normalized spectra were transformed from energy to k-space and further weighted by k^3 to distinguish the contributions of backscattering interferences from different coordination shells. Normally, the backscattered amplitude and phase shift functions for specific atom pairs were theoretically estimated by utilizing the FEFF8.0 code. The X-ray photoelectron spectroscopy (XPS) (Thermo VG Scientific Sigma Probe, operated at a voltage of 20 kV and a current of 30 mA) with a monochromatic X-ray source (Al K α) was employed to investigate the oxidation states and surface compositions of the experimental samples. The surface compositions of the samples were estimated by calculating the integral of each peak. Shirley-type background was used to subtract the original peak, and then a combination of Lorentzian and Gaussian lines was applied to fit the experimental curve. Accurate binding energies were determined by reference to the C 1s peak at 284.6 eV.

3. Electrochemical Analysis

The electrochemical measurements were carried out at room temperature using a potentiostat (CH Instruments Model 600B, CHI 600B) equipped with a three-electrode system. The catalyst slurry was prepared by ultrasonic dispersion of 5 mg catalyst powder in 1.0 ml of isopropanol (IPA) and 50 μl of Nafion-117 (99%, Sigma-Aldrich Co.). For conducting the electrochemical measurements, 10.0 μl of catalyst slurry was dropped and air-dried on a glassy carbon rotating disk electrode (RDE) (0.196 cm^2 area) as a working electrode. Hg/HgCl₂ (the voltage was calibrated by 0.242 V, in alignment with that of RHE) electrode saturated in KCl aqueous solution was used as the reference electrode. Whereas, a Pt wire was employed as the counter electrode. The cyclic voltammetry (CV) curves were obtained at the voltage scan rate of 0.02 V s^{-1} and the potential range of 0.1 V to 1.3 V (V vs RHE.) in an N₂ saturated 0.1 M KOH electrolyte (pH 13). Besides, Ag/AgCl electrode were used as the reference electrode for CO-stripping analysis. The adsorption of CO on the surface of the catalyst was performed by purging CO into 0.5 M H₂SO₄ at 0.05 V (vs NHE) for 20 min. Then the CO stripping voltammetry was measured between -0.10 and 1.20 V (vs NHE) in N₂ saturated 0.5 M H₂SO₄ solution at a scan rate of 50 mVs^{-1} .

4. Gaseous Product Analysis

The catalytic performances of experimental samples were assessed by using the previously reported protocol.¹⁻² **Scheme 1a** and **1b** depicts the experimental setup for gaseous product analysis, while the reaction conditions are shown in **Scheme 1c**. For calibration purpose, the standard gases including H₂ and CO (each 200 ppm), as well as CH₄, C₂H₆ and C₃H₈ (each 100 ppm) balanced in “He” were purchased from ECGAS Asia (Taiwan). The different concentrations of the aforementioned gases were prepared by introducing gases into sampling loops of various sizes. The gas cylinder was directly connected to the 6-port switching valve to fill the sampling loop which is later injected into the GC column. The gas samples were directly collected from the thermal catalytic reactor to evaluate the performance. The experiment is performed with an automatic premixed gas supply apparatus equipped with a heating block for the chosen catalyst to be packed within a glass tube to form a thermal reaction bed. The length and thickness of glass tube packed with catalyst are 100 mm and 1 mm, respectively, while the inside diameter is 2 mm. The temperature of the reaction bed was adjusted by a thermal controller with a PID algorithm, which allowed users to set up an analytical method with the desired reaction time, temperature and flow rate, as well as to remote-start a GC with self-designed software as the interface. The total flow rate of the gases was measured and controlled by a mass flow controller (MFC). All gaseous samples coming from the reaction bed were analyzed by a gas chromatograph (GC) (Agilent 7890, USA) instrument equipped with a Valco PDHID detector (model D-3-I-7890, VICI, USA) and a micro packed column packed with carbon molecular sieve (Shincarbon ST, 2 m x 1.0 mm i.d.; Restek Chromatography Products, USA). The gas samples are introduced into the GC column by the 6 port switching valve (A6C6UWT, VICI) from the sampling loop to inject a fixed volume of sample (160 μL). Ultra-high-purity helium (UHP) (99.9995%) is used as both the carrier gas and discharge gas, while two heated helium purifiers (HP2 and HPM, VICI, USA) are placed between the cylinder and the flow splitter to remove impurities in the UHP helium and to stabilize the baseline. The helium flow rate is 30 ml/min regulated by a restrictor (30 cc/min 60 psi He, VICI). The constant pressure mode of the carrier gas is set at 90 psi controlled by a pressure control module (PCM, Agilent). The oven temperature is programmed from 308 K (1.5 min) to 553 (ramping at 20 K/min) holding for 3.25 min. Stainless steel tubing is used throughout the thermal reactor and GC's sampling system. All the connectors have been tested for leaks with an electric leak detector. The catalytic reaction bed is enclosed in a heating block operated at near-atmosphere pressure. Twelve mg of the catalyst is mixed with 23 mg of silica gel (60/80 mesh, Alltech, USA) and then placed inside a glass tube (2 mm ID × 3 mm OD, 100 mm length) with quartz wool plugs at both ends. As the first step, N₂ gas (50 mL/min) was introduced into the reactor bed at RT for one hour to remove moisture in the catalyst, followed by feeding gas of pure CO₂ or CO₂ – H₂ mixture (CO₂ : H₂ = 1 : 3) at 20 mL/min to the reaction bed in the temperature ranging from 323 to 573 K. After 30 min at isothermal temperature, gas products are injected into the analytic column from the sampling loop for GC analysis. The sensitivity of the detection system is up to ~0.1 ppm.



Scheme 1. Schematic diagram of (a) the experimental apparatus for an automatic premixed gas supply equipped with a catalyst-packed thermal reaction bed. (b) the catalyst reaction bed by pacing a chosen catalyst into a glass tube. The tube is enclosed within a heating block. (c) The schematic representation of reaction conditions.

5. Digital Image Processing Analysis of CoOx@Pd.

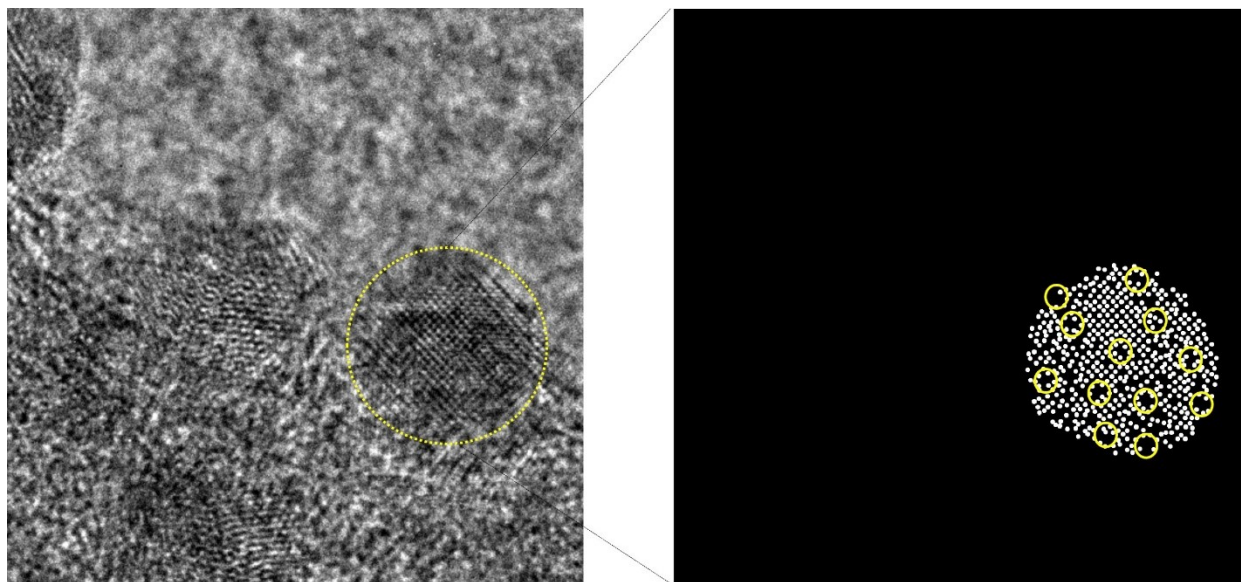


Figure S1. The HRTEM images of CoOx@Pd and the corresponding image processing result. The defect sites are denoted by yellow circles.

6. Model analysis fitting curves compared with experimental FT-EXAFS spectra at Co K-edge.

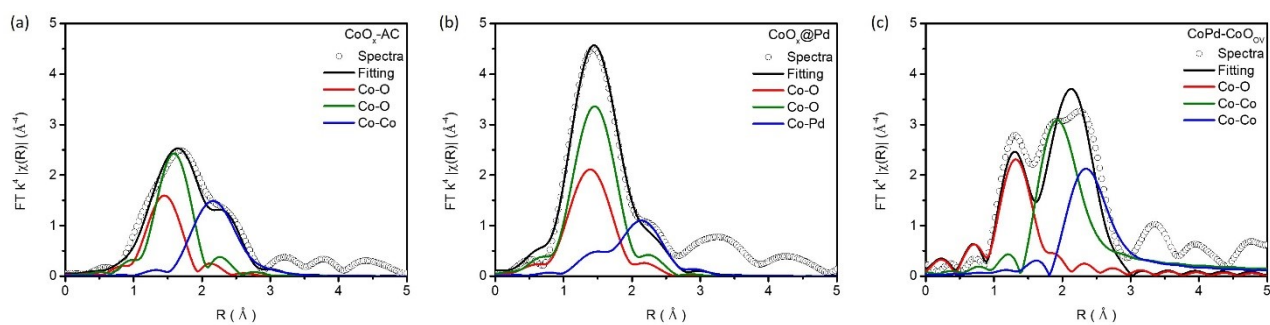


Figure S2. Model analysis fitting curves compared with experimental FT-EXAFS spectra at Co K-edge of (a) CoO_x-AC, (b) CoO_x@Pd, and (c) CoPd-CoO_{ov}.

7. XANES and FT-EXAFS spectra of the CoPd-CoO_{OV} NC compared with reference samples (Pd-foil, Pd-AC and CoO_x@Pd) at the Pd K-edge.

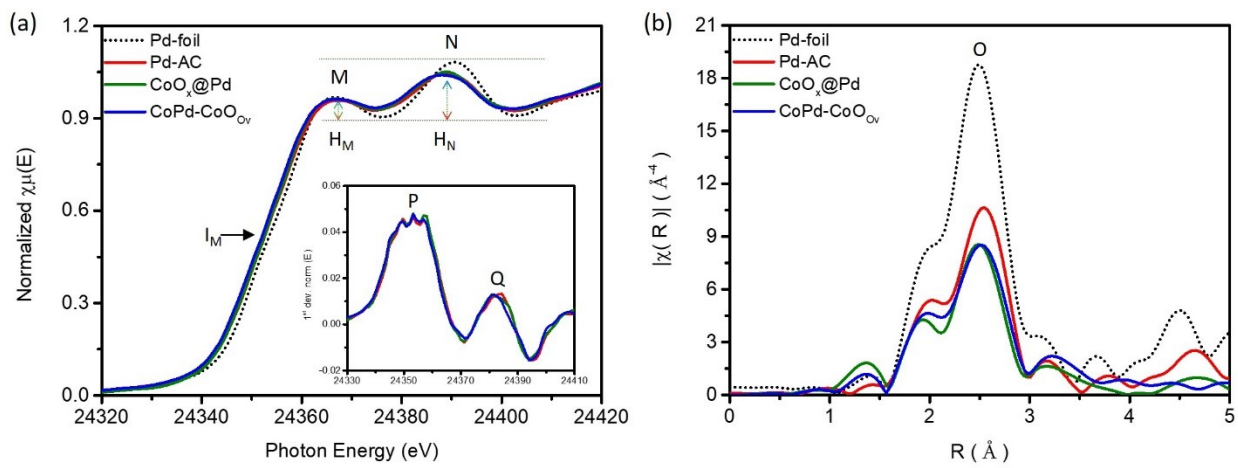


Figure S3. (a) XANES and (b) FT-EXAFS spectra of the CoPd-CoO_{OV} NC compared with reference samples (Pd-foil, Pd-AC and CoO_x@Pd) at the Pd K-edge.

8. Model analysis fitting curves compared with experimental FT-EXAFS spectra at Pd K-edge.

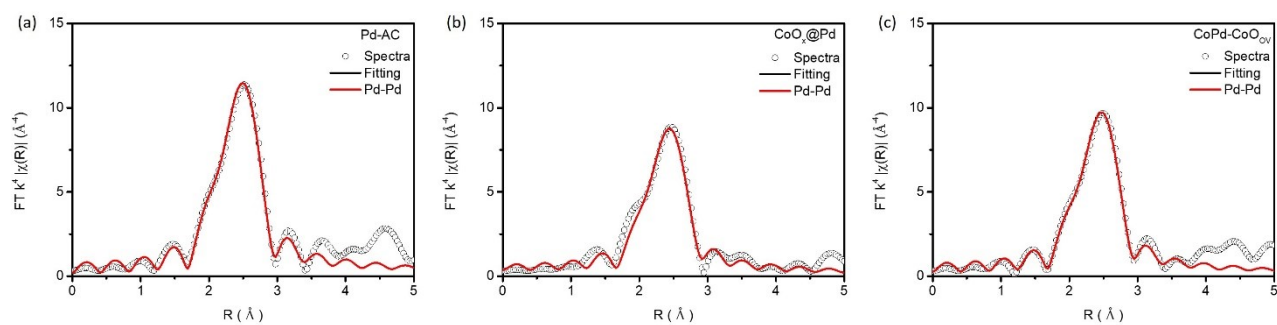


Figure S4. Model analysis fitting curves compared with experimental FT-EXAFS spectra at Pd K-edge of (a) Pd-AC, (b) CoO_x@Pd, and (c) CoPd-CoO_{ov}.

9. Inductively coupled plasma-atomic emission spectrometer (ICP-AES) determined chemical composition of experimental NCs.

Table S1. Inductively coupled plasma-atomic emission spectrometer (ICP-AES) determined chemical composition of experimental NCs.

Samples	Co (wt.%)	Pd (wt.%)
CoO _x @Pd	10.07	18.98
CoPd-CoO _{OV}	14.53	19.03

10. XPS determined elemental chemical states and binding energies of experimental NCs.

Table S2. XPS determined elemental chemical states of experimental NCs.

Catalyst	Elemental chemical states (%)								Ratio		Composition		
	Co-Pd	Co ²⁺	Co ³⁺	C-O	C=O	O _V	O _L	Pd ²⁺	Pd ⁰	Co ²⁺ /Co ³⁺	O _V /O _L	Co	Pd
CoOx@Pd	25.0	31.4	43.6	25.5	36.5	30.7	7.3	43.68	56.32	1.29	4.21	62.59	37.41
CoPd-CoO _{OV}	23.4	42.2	34.4	23.5	36.8	32.9	6.8	37.87	62.13	1.91	4.84	77.47	22.53

Table S3. XPS determined binding energies of experimental NCs.

Catalyst	Binding Energy (eV)								
	Co-Pd	Co ²⁺	Co ³⁺	C-O	C=O	O _V	O _L	Pd ²⁺	Pd ⁰
CoOx@Pd	783.58	782.45	781.27	533.88	532.74	531.94	531.17	336.11	334.84
CoPd-CoO _{OV}	783.53	782.16	780.97	534.07	532.90	531.94	530.62	337.19	335.70

References

1. C. Yan, C.-H. Wang, M. Lin, D. Bhalothia, S.-S. Yang, G.-J. Fan, J.-L. Wang, T.-S. Chan, Y.-l. Wang, X. Tu, S. Dai, K.-W. Wang, J.-H. He and T.-Y. Chen, *Journal of Materials Chemistry A*, 2020, **8**, 12744-12756.
2. D. Bhalothia, W.-H. Hsiung, S.-S. Yang, C. Yan, P.-C. Chen, T.-H. Lin, S.-C. Wu, P.-C. Chen, K.-W. Wang, M.-W. Lin and T.-Y. Chen, *ACS Applied Energy Materials*, 2021, **4**, 14043-14058.